

Homogeneous cooling of mixtures of particle shapes

R. C. Hidalgo, D. Serero, and T. Pöschel

Citation: *Physics of Fluids* **28**, 073301 (2016); doi: 10.1063/1.4954670

View online: <http://dx.doi.org/10.1063/1.4954670>

View Table of Contents: <http://scitation.aip.org/content/aip/journal/pof2/28/7?ver=pdfcov>

Published by the [AIP Publishing](#)

Articles you may be interested in

[Homogeneous states in driven granular mixtures: Enskog kinetic theory versus molecular dynamics simulations](#)

J. Chem. Phys. **140**, 164901 (2014); 10.1063/1.4871628

[From discrete particles to continuum fields in mixtures](#)

AIP Conf. Proc. **1542**, 1202 (2013); 10.1063/1.4812153

[A hierarchy of particle-size segregation models: From polydisperse mixtures to depth-averaged theories](#)

AIP Conf. Proc. **1542**, 66 (2013); 10.1063/1.4811869

[Continuum representation of a continuous size distribution of particles engaged in rapid granular flow](#)

Phys. Fluids **24**, 083303 (2012); 10.1063/1.4744987

[Instabilities in the homogeneous cooling of a granular gas: A quantitative assessment of kinetic-theory predictions](#)

Phys. Fluids **23**, 093303 (2011); 10.1063/1.3633012

The banner features a blue background with a bright light source on the right, creating a lens flare effect. On the left, there is a small image of a book cover for 'AIP Applied Physics Reviews' with a technical diagram. The main text 'NEW Special Topic Sections' is in large, white, bold font. Below it, 'NOW ONLINE' is in yellow, followed by 'Lithium Niobate Properties and Applications: Reviews of Emerging Trends' in white. The AIP Applied Physics Reviews logo is in the bottom right corner.

NEW Special Topic Sections

NOW ONLINE
Lithium Niobate Properties and Applications:
Reviews of Emerging Trends

AIP Applied Physics Reviews

Homogeneous cooling of mixtures of particle shapes

R. C. Hidalgo,¹ D. Serero,² and T. Pöschel²

¹*Departamento de Física y Matemática Aplicada, Facultad de Ciencias, Universidad de Navarra, 31080 Pamplona, Spain*

²*Institut für Multiskalensimulation, Friedrich-Alexander-Universität Erlangen-Nürnberg, Erlangen, Germany*

(Received 7 December 2015; accepted 12 June 2016; published online 1 July 2016)

In this work, we examine theoretically the cooling dynamics of binary mixtures of spheres and rods. To this end, we introduce a generalized mean field analytical theory, which describes the free cooling behavior of the mixture. The relevant characteristic time scale for the cooling process is derived, depending on the mixture composition and the aspect ratio of the rods. We simulate mixtures of spherocylinders and spheres using a molecular dynamics algorithm implemented on graphics processing unit (GPU) architecture. We systematically study mixtures composed of spheres and rods with several aspect ratios and varying the mixture composition. A homogeneous cooling state, where the time dependence of the system's intensive variables occurs only through a global granular temperature, is identified. We find cooling dynamics in excellent agreement with Haff's law, when using an adequate time scale. Using the scaling properties of the homogeneous cooling dynamics, we estimated numerically the efficiency of the energy interchange between rotational and translational degrees of freedom for collisions between spheres and rods. *Published by AIP Publishing.* [<http://dx.doi.org/10.1063/1.4954670>]

I. INTRODUCTION

Granular gases are ensembles of macroscopic particles that lose energy due to their non-elastic collisions. Thus, the continuous energy dissipation keeps them mainly out of thermal equilibrium, and only when an external energy source is involved, a steady state can be reached.^{1,2} Over the last decades, granular gases have been thoroughly examined analytically,^{1,2} experimentally,³⁻⁸ and numerically.^{1,2} Hence, it has been proven that a freely evolving, weak dissipative gas cools down homogeneously, reaching the so-called homogeneous cooling state (HCS).^{9,10} In those conditions, the particles are uniformly distributed in space and the cooling dynamics is governed by the granular temperature, which is proportional to the average kinetic energy.

Kinetic analytical theories and hydrodynamic approaches have been developed to describe the macroscopic properties of granular gases.^{1,2} Hence, it is well accepted that both the cooling dynamics and the process characteristic time are determined by the inelasticity of the particles and the frequency of collision.^{11,12} For instance, when considering the most simple case, an ensemble of spherical particles with constant restitution coefficient, the granular temperature diminishes following Haff's law resulting in an asymptotic decay $T(t) \sim t^{-2}$.¹³ Meanwhile, when particle interaction is characterized by a velocity dependent restitution coefficient, a generalized cooling law can be deduced.^{1,2} For the particular case of a Hertz-contact, the asymptotic algebraic decay of the granular temperature reduces to $T(t) \sim t^{-5/3}$.¹⁴

Nevertheless, it is very well known that at large time scales, the HCS becomes unstable and the system subsequently evolves into an inhomogeneous state, while the cooling process notably slows down.¹⁵⁻¹⁸ In this regime, the particles' collective motion determines the system behavior, and large density inhomogeneities are typically observed.¹⁵⁻¹⁸ Hence, clusters of particles appear, grow, and interact due to dissipative collisions.¹⁸ Moreover, it is also known that particle friction plays a crucial role in the cooling dynamics of granular gases. Particle roughness induces a non-trivial energy interchange, which leads to a complicated energy sharing among degrees of freedom.¹⁹⁻²² In

general, the time evolution of the rotational and translational kinetic energies is coupled; however, no full equipartition between degrees of freedom is commonly found.^{19–22}

The effect of particle shape on the kinetic evolution of granular gases has been explored a long time ago.^{23,24} Zippelius and coworkers developed a kinetic theory of hard needles based on the assumption of a HCS. Thus, it was found that the energy interchange between degrees of freedom is controlled by the macroscopic restitution coefficient and by the distribution of mass along the needles.²³ More recently, there is an increasing interest in the cooling dynamics of non-spherical grains both experimentally^{6–8} and numerically.^{25–28} Here, the primary interest is also focused on the time evolution of the translational and rotational kinetic energies. Normally, in granular gases of elongated particles, equipartition does not apply. Moreover, it has been found that several details of the cooling process depend on particle aspect ratio, mass distribution of the grains, and the driving mechanisms.^{25–28}

In addition to their deviation from perfect spherical shape, realistic granular materials are polydisperse. This feature is the source of interesting, and often counter-intuitive effects,^{29–31} regarding, e.g., their mixing/segregation properties, of which the Brazil nut effect³² constitutes perhaps the most famous illustration. In the realm of granular gases, a number of hydrodynamic descriptions have been derived for inelastic binary mixtures^{33–35} based on the analysis of the appropriate Boltzmann equations. In the simpler case of a homogeneous binary mixture, studies have shown the existence of a homogeneous cooling state,^{34–38} and the analysis of the cooling properties of those systems has revealed, in particular, the potential breakdown of the energy equipartition between species, similar to what can be observed in systems possessing internal degrees of freedom. All of those studies deal however (in 3 dimensions) with spherical particles, whether smooth (in the vast majority of the works) or rough²² case.

The purpose of the present work is to investigate the cooling properties of systems combining both non-spherical shape and polydispersity, by considering a homogeneous mixture of spheres and rods. The paper is organized as follows: in Sec. II we introduce some basic concepts about the kinetics of a dilute granular mixture composed of rods and spheres, in Sec. III we briefly describe the numerical model and implementation of our algorithm, and Sec. III discusses the numerical results of the homogeneous cooling of our system. At the end, conclusions and outlook are drawn.

II. HOMOGENEOUS COOLING STATE, MIXTURE OF SPHERES AND RODS

Consider a binary mixture of smooth spheres and rods of mass m , having number densities n_S and n_R , respectively (see sketch in Fig. 1). The smoothness of the particles render irrelevant rotational degrees of freedom of the spheres, as well as the rotation of the rods around their axis, so that the angular momentum of rods is characterized by a single (for symmetry reasons) moment of inertia I , corresponding to the rotation around a direction perpendicular to the axis. From a kinetic point of view, the mixture is described by a set of two distribution functions, $f_R(\mathbf{v}, \boldsymbol{\omega}, \gamma)$ and $f_S(\mathbf{v})$, corresponding to the rods and the spheres, respectively, where \mathbf{u} denotes the velocity of the (center of mass of the) particles, $\boldsymbol{\omega}$ the angular velocity of the rods, and γ denotes the angular orientation of the rod axis. From the hydrodynamic point of view, in addition to the number density, the system is described by three granular temperatures, describing (internal) translational and rotational average energies, given in terms of the distribution functions (in the absence of convection) by

$$T_S \equiv \frac{1}{n_S} \int f_S(\mathbf{u}) m \mathbf{u}^2 d\mathbf{v},$$

for the translational kinetic energy of the spheres,

$$T_R = \frac{1}{n_R} \int f_R(\mathbf{u}, \boldsymbol{\omega}, \gamma) m \mathbf{u}^2 d\mathbf{v} d\boldsymbol{\omega} d\gamma,$$

for the translational kinetic energy of the rods, and

$$\theta_R = \frac{1}{n_R} \int f_R(\mathbf{u}, \boldsymbol{\omega}, \gamma) I \boldsymbol{\omega}^2 d\mathbf{u} d\boldsymbol{\omega} d\gamma,$$

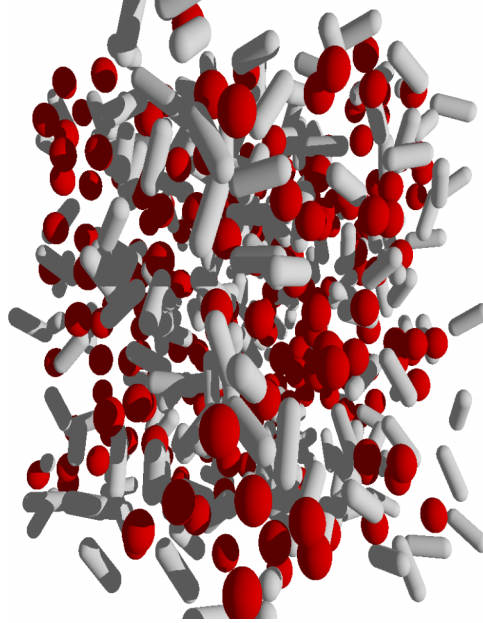


FIG. 1. Dilute mixtures of spheres and spherocylinders with aspect ratio of $\xi = 3$. We illustrate a system with $N = 512$ and $\beta = 0.5$.

for the rotational kinetic energy of the rods. The overall mixture temperature of the mixture is defined as

$$T = (1 - \beta)T_S + \beta T_R + \beta \theta_R, \quad (1)$$

where $\beta \equiv \frac{n_R}{n}$, and $n \equiv n_S + n_R$. Notice that the temperatures are *not* defined per degree of freedom, but as (twice) the energy per particle. We consider the behavior of a mixture in the Homogeneous Cooling State (HCS),^{13,39} whose dynamics is driven by its energy, described by the equation for T ,

$$n \frac{\partial T}{\partial t} = -\Gamma, \quad (2)$$

where Γ is the cooling rate, describing the decay of energy due to the inelastic nature of the collisions, and comprises three contribution corresponding to sphere-sphere, sphere-rod, and rod-rod collisions,

$$\begin{aligned} \Gamma = & \int f_S(\mathbf{u}_1) f_S(\mathbf{u}_2) |\mathbf{u}_{12}| \Delta E_{SS} ds_{SS} d\mathbf{u}_1 d\mathbf{u}_2 + 2 \int f_S(\mathbf{u}_1) f_R(\mathbf{u}_2, \omega_2, \gamma) |\mathbf{u}_{12}| \Delta E_{RS} ds_{RS} d\mathbf{u}_1 d\mathbf{u}_2 d\omega_2 d\gamma \\ & + \int f_R(\mathbf{u}_1, \omega_1, \gamma_1) f_R(\mathbf{u}_2, \omega_2, \gamma_2) |\mathbf{u}_{12}| \Delta E_{RR} ds_{RR} d\mathbf{u}_1 d\mathbf{u}_2 d\omega_1 d\omega_2 d\gamma_1 d\gamma_2, \end{aligned} \quad (3)$$

where ds_{SS} , ds_{RS} , and ds_{RR} are the differential cross sections corresponding to sphere-sphere, sphere-rod, and rod-rod collisions, respectively, $\mathbf{u}_{12} \equiv \mathbf{u}_1 - \mathbf{u}_2$ is the relative velocity of the centers of mass of the colliding particles, and ΔE_{SS} , ΔE_{RS} , ΔE_{RR} are the energy losses in the three types of collisions. For constant coefficients of restitution (see more below), in the case of hard spheres (or disks), solving Eq. (3) results in Haff's law¹³ describing the dynamics of the temperature field,

$$T(t) = \frac{T(0)}{\left(1 + \frac{\Gamma(0)}{2T(0)}t\right)^2}. \quad (4)$$

The cooling coefficient Γ has been recently evaluated for a monodisperse system of ellipsoids, by employing the (elastic) equilibrium expression for the collision frequency, and extrapolating the formula derived for disk and spheres to five dimensions,²⁵ to account for the additional rotational degrees of freedom. Note that full energy equipartition is, however, a property of equilibrium, a

state that cannot be reached by a granular gas, because of the dissipative nature of the interactions between the grains. For instance, equipartition is known to break down in the case of, e.g., inelastic rough disks and spheres,^{40,41} mixtures of granular gases,^{33,34,36} or hard needles.²³ We therefore proceed here to extend the evaluation of the cooling coefficient to the case of binary mixtures of rods and spheres, relaxing the assumption of equipartition.

A. Dynamics of collisions

Consider the collision of two rigid biaxial bodies, labeled “1” and “2.” The velocities of the particles at the point of contact are given by

$$\begin{aligned}\mathbf{c}_1 &= \mathbf{u}_1 + \boldsymbol{\omega}_1 \times \mathbf{r}_1, \\ \mathbf{c}_2 &= \mathbf{u}_2 + \boldsymbol{\omega}_2 \times \mathbf{r}_2,\end{aligned}$$

where \mathbf{r}_1 and \mathbf{r}_2 are the vectors joining the centers of the particles to the contact point. Define \mathbf{n} as the unit vector normal to the surface (pointing from 1 to 2) at contact. The coefficient of normal restitution α is defined by

$$\mathbf{c}'_{12} \cdot \mathbf{n} = -\alpha \mathbf{c}_{12} \cdot \mathbf{n}, \quad (5)$$

where $\mathbf{c}_{12} \equiv \mathbf{c}_1 - \mathbf{c}_2$ is the relative velocity at contact, and primes denote post-collisional quantities. The post-collisional angular momenta around the centers of mass are

$$\begin{aligned}\mathbf{J}'_1 &= \mathbf{J}_1 + \mathbf{r}_1 \times \Delta \mathbf{p}_{12}, \\ \mathbf{J}'_2 &= \mathbf{J}_2 - \mathbf{r}_2 \times \Delta \mathbf{p}_{12},\end{aligned}$$

where $\Delta \mathbf{p}_{12}$ is the change of momentum of particle “1” in collision, and \mathbf{J}_1 and \mathbf{J}_2 are the pre-collisional angular momenta of the colliding bodies. For symmetry reasons, since the absence of friction makes the rotation around the axis of the bodies irrelevant, the angular momenta can be taken proportional to the angular velocities: $\mathbf{J}_1 = I_1 \boldsymbol{\omega}_1$; $\mathbf{J}_2 = I_2 \boldsymbol{\omega}_2$, with I_1 and I_2 the moment of inertia of the particles around a direction perpendicular to their axis. Therefore,

$$\begin{aligned}\boldsymbol{\omega}'_1 &= \boldsymbol{\omega}_1 + \frac{\mathbf{r}_1 \times \Delta \mathbf{p}_{12}}{I_1}, \\ \boldsymbol{\omega}'_2 &= \boldsymbol{\omega}_2 - \frac{\mathbf{r}_2 \times \Delta \mathbf{p}_{12}}{I_2}.\end{aligned}$$

Using the fact that $\Delta \mathbf{p}_{12} = \Delta p_{12} \mathbf{n}$ (no tangential force), together with Eq. (5), one obtains

$$\Delta p_{12} = -\frac{(1 + \alpha)}{2} \frac{\mathbf{c}_{12} \cdot \mathbf{n}}{\frac{1}{m} + \frac{1}{2} \left(\frac{(\mathbf{r}_1 \times \mathbf{n})^2}{I_1} + \frac{(\mathbf{r}_2 \times \mathbf{n})^2}{I_2} \right)}.$$

Using the above expression for Δp_{12} one can readily obtain the following expression for the change of kinetic energy in collision:

$$\Delta E_{12} = -\frac{(1 - \alpha^2)}{4} \mu(\mathbf{r}_1, \mathbf{r}_2, \mathbf{n}) (\mathbf{c}_{12} \cdot \mathbf{n})^2, \quad (6)$$

where

$$\frac{1}{\mu} \equiv \frac{1}{m} \left(1 + \frac{m}{2} \left(\frac{(\mathbf{r}_1 \times \mathbf{n})^2}{I_1} + \frac{(\mathbf{r}_2 \times \mathbf{n})^2}{I_2} \right) \right).$$

The energy losses in the three types of collision are thus given by

$$\Delta E_{RR} = -\frac{(1 - \alpha^2)}{4} \frac{m(\mathbf{c}_{12} \cdot \mathbf{n})^2}{1 + \frac{m}{2I} \left((\mathbf{r}_1 \times \mathbf{n})^2 + (\mathbf{r}_2 \times \mathbf{n})^2 \right)}, \quad (7)$$

for rod-rod collisions,

$$\Delta E_{RS} = -\frac{(1 - \alpha^2)}{4} \frac{m(\mathbf{u}_{12} \cdot \mathbf{n} + (\boldsymbol{\omega}_1 \times \mathbf{r}_1) \cdot \mathbf{n})}{\left(1 + \frac{m}{2I} (\mathbf{r}_1 \times \mathbf{n})^2 \right)}, \quad (8)$$

for rod-spheres collisions, where index “1” pertains to the rod, and

$$\Delta E_{RR} = -\frac{1 - \alpha^2}{4} m(\mathbf{u}_{12} \cdot \mathbf{n})^2,$$

for sphere-sphere collisions.

B. Cooling coefficient

In order to evaluate Γ (cf. Eq. (3)), one needs expressions for the distribution functions f_1 and f_2 , which requires solving the relevant set of coupled Boltzmann equations. For the sake of simplicity, we consider here normal distributions (i.e., which depend on time only through the temperature) and approximate f_1 and f_2 by Maxwellian distributions. As mentioned, equipartition cannot *a priori* be assumed, and we therefore consider the following ansatz for the distribution functions, where the (two) translational velocities and rotational velocities are scaled with different temperatures,

$$f_1(\mathbf{u}_1, \omega_1, \gamma_1) = \frac{n_1}{\Omega} \left(\frac{3m}{2\pi T_{R1}} \right)^{\frac{3}{2}} \left(\frac{I_1}{\pi\theta_1} \right) e^{-\left(\frac{3mu_1^2}{2T_{R1}} + \frac{I_1\omega_1^2}{\theta_1} \right)}, \tag{9}$$

$$f_2(\mathbf{u}_2, \omega_2, \gamma_2) = \frac{n_2}{\Omega} \left(\frac{3m}{2\pi T_{R2}} \right)^{\frac{3}{2}} \left(\frac{I_2}{\pi\theta_2} \right) e^{-\left(\frac{3mu_2^2}{2T_{R2}} + \frac{I_2\omega_2^2}{\theta_2} \right)}, \tag{10}$$

where $\Omega = \int d\gamma = 4\pi$. Notice that assuming a normal solution implies that, while the temperatures T_{R1} , T_{R2} , θ_1 , and θ_2 are different from each other, their dynamics remain enslaved to that of T , and all temperature ratios are constant in time. For the homogeneous cooling state of a binary mixture of inelastic spheres, similar assumptions have been shown to yield accurate results.^{34,36} With the above assumptions, the cooling coefficient Γ is given by (see Appendix for details),

$$\Gamma = (1 - \alpha^2)n \frac{T^{3/2}}{\sqrt{m}} \tilde{\Gamma}, \tag{11}$$

where

$$\begin{aligned} \tilde{\Gamma} = & -\frac{\sqrt{3}}{9\sqrt{\pi}} \left[\beta^2 \left(\frac{T_R}{T} \right)^{\frac{3}{2}} \left\langle \frac{\left(1 + \frac{3m}{4I} \left(\frac{\theta}{T_R} (\mathbf{r}_1 \times \mathbf{n})^2 + \frac{\theta}{T_R} (\mathbf{r}_2 \times \mathbf{n})^2 \right) \right)^{\frac{3}{2}}}{1 + \frac{m}{2I} \left((\mathbf{r}_1 \times \mathbf{n})^2 + (\mathbf{r}_2 \times \mathbf{n})^2 \right)} \right\rangle_{RR} \right. \\ & \left. + 2\beta(1 - \beta) \left(\frac{T_R + T_S}{2T} \right)^{\frac{3}{2}} \left\langle \frac{\left(1 + \frac{3m}{2I} \frac{\theta}{T_R + T_S} (\mathbf{r}_1 \times \mathbf{n})^2 \right)^{\frac{3}{2}}}{1 + \frac{m}{2I} (\mathbf{r}_1 \times \mathbf{n})^2} \right\rangle_{RS} + (1 - \beta)^2 \left(\frac{T_S}{T} \right)^{\frac{3}{2}} \langle 1 \rangle_{SS} \right]. \tag{12} \end{aligned}$$

The brackets in Eq. (12) are defined as

$$\begin{aligned} \langle \Phi \rangle_{RR} &= \frac{1}{\Omega^2} \int_{RR} \Phi S_{RR}(\mathbf{n}, \gamma_1, \gamma_2) d\mathbf{n} d\gamma_1 d\gamma_2, \\ \langle \Phi \rangle_{RS} &= \frac{1}{\Omega^2} \int_{RS} \Phi S_{RS}(\mathbf{n}, \gamma_1, \gamma_2) d\mathbf{n} d\gamma_1 d\gamma_2, \\ \langle \Phi \rangle_{SS} &= \frac{1}{\Omega^2} \int_{SS} \Phi S_{SS}(\mathbf{n}, \gamma_1, \gamma_2) d\mathbf{n} d\gamma_1 d\gamma_2, \end{aligned}$$

where $S_{RR}(\mathbf{n}, \gamma_1, \gamma_2)$, $S_{RS}(\mathbf{n}, \gamma_1, \gamma_2)$, $S_{SS}(\mathbf{n}, \gamma_1, \gamma_2)$, and the integration domains of \mathbf{n} correspond to excluded volume, according to the type of collisions and depending on the orientation of the particles. In particular, for a collision between hard spheres, $\langle 1 \rangle_{SS} = \int \sigma^2 d\mathbf{n} = 4\pi\sigma^2$. As mentioned, in a normal state, all temperature ratios are constant in time, so that the dependence of Γ (cf. Eq. (11)) on T ($\Gamma \propto T^{3/2}$) yields Haff’s law, cf. Eq. (4).

We can proceed to evaluate Eq. (12) in the limiting case of energy equipartition between species and degrees of freedom,

$$T_R = T_S = \frac{3}{2}\theta, \quad (13)$$

$$T = \left((1 - \beta) + \frac{5}{3}\beta \right) T_R, \quad (14)$$

and the cooling coefficient, Eq. (12), reduces to

$$\tilde{\Gamma}_o = \frac{\beta^2 \mathcal{D}_{RR} + 2\beta(1 - \beta) \mathcal{D}_{RS} + (1 - \beta)^2 4\pi\sigma^2}{\sqrt{\pi}(2\beta + 3)^{3/2}}, \quad (15)$$

where

$$\mathcal{D}_{RR} \equiv \left\langle \sqrt{1 + \frac{m}{2I} \left((\mathbf{r}_1 \times \mathbf{n})^2 + (\mathbf{r}_2 \times \mathbf{n})^2 \right)} \right\rangle_{RR}$$

describes the efficiency of the energy interchange between rotational and translational degrees of freedom in rod-rod collisions, while

$$\mathcal{D}_{RS} \equiv \left\langle \sqrt{1 + \frac{m}{2I} (\mathbf{r}_1 \times \mathbf{n})^2} \right\rangle_{RS},$$

accounts for the energy interchange in collisions between rods and spheres. Setting $\beta = 1$ in Eq. (15), the analytical results corresponding to a mono-disperse gas of ellipsoids^{25,26} and rods,⁴⁵ which were derived assuming (implicitly) equipartition, are recovered. Notice that, in contrast to the present analysis, the evaluation of $\tilde{\Gamma}_o$ for a monodisperse system of frictionless ellipsoids in Ref. 25 was based on an extrapolation of the formula pertaining to frictionless spheres to five dimensions, corresponding to two rotational and three translational degrees of freedom.

III. NUMERICAL MODEL

In this work, we improve a hybrid GPU-CPU discrete element algorithm for simulating three-dimensional spherical⁴⁶ and non-spherical^{26,45} particles that were recently introduced. Here we examine mixtures of particles made of the same material but with different shapes, specifically, spheres and rods. In the model, the rods are described as spherocylinders, which are characterized by their length l , sphero-radius r , the volume $V_p = \pi r^2 l + \frac{4}{3}\pi r^3$, and the aspect ratio $\xi = \frac{l+2r}{2r}$. For the sake of simplicity, we consider a mixture with spherical particles with the same volume V_p . Accordingly, the radius of the spherical particles is $\sigma = \left(\frac{V_p}{4/3\pi} \right)^{\frac{1}{3}}$. The system composition is characterized by the weighting parameter β , which is defined as the ratio of the total number of rods N_{rd} to the total number of particles in the mixture N_T , $\beta = \frac{N_{rd}}{N_T}$. Accordingly, the number of spherical particles in the system is $N_s = (1 - \beta)N_T$.

To calculate the particle-particle interaction, we use an efficient algorithm for interacting spheropolyhedra,^{47,48} implemented on GPU architecture,⁴⁵ which allows to describe systems with large number of particles in 3D. The only new ingredient is taking into account the type of interacting particles (sphere-sphere, sphere-rod, and rod-rod), to properly define the plane of contact and the overlap distance. In the new algorithm, the particles are labeled. The three possible types of contact are illustrated on the sketch of Fig. 2. Note that both the magnitude of the force and the direction of the contact plane depend only on the local inter-penetration between the two contacting spheres.^{47,49} Moreover, as the particles are considered friction-less, the contact force always acts normal to the plane of contact \hat{n} . The contact force has an elastic and a dissipative contribution, $\mathbf{F}_{ij} = -k^n \delta \hat{n} - \gamma^n v_{rel}^n \hat{n}$, where δ accounts for the overlap distance, k^N is the spring constant, γ^n is the damping coefficient, and v_{rel}^n represents the normal relative velocity between the particles.

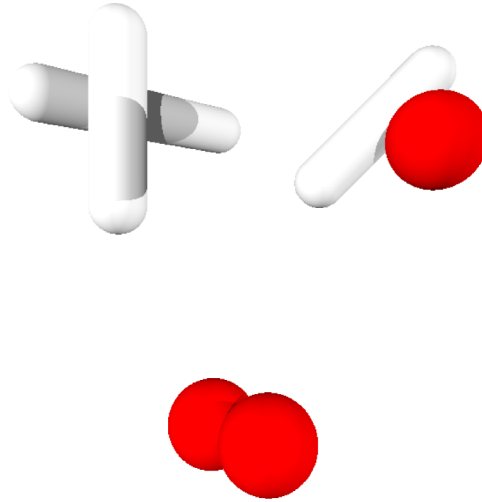


FIG. 2. Sketch of the three types of collision within the system. Note that particle volume and mass is kept the same for both types of particle.

We have numerically solved the Newton's equation of motion of each particles i ($i = 1, \dots, N$) of the mixture,

$$\sum_{j=1}^{N_c} \mathbf{F}_{ij} = m\ddot{\mathbf{r}}_i, \quad (16)$$

for the translation degrees of freedom. Moreover, particularly for the rods particles, the *Euler's* equations that describe their rotational motion,

$$\begin{aligned} \sum_{j=1}^{N_c} \tau_{ij}^x &= M_i^x = I_{xx} \dot{\omega}_i^x - (I_{yy} - I_{zz}) \omega_i^y \omega_i^z, \\ \sum_{j=1}^{N_c} \tau_{ij}^y &= M_i^y = I_{yy} \dot{\omega}_i^y - (I_{zz} - I_{xx}) \omega_i^z \omega_i^x, \\ \sum_{j=1}^{N_c} \tau_{ij}^z &= M_i^z = I_{zz} \dot{\omega}_i^z - (I_{xx} - I_{yy}) \omega_i^x \omega_i^y, \end{aligned} \quad (17)$$

are also numerically solved. In these expressions, m represents the particles' mass, which is the same for both types. I_{xx} , I_{yy} , I_{zz} are the eigen-values of the moment of inertia tensor I_{ij} of a spherocylinder. Note that \mathbf{F}_{ij} is the force exerted by particle j on particle i and τ_{ij} is the corresponding torque. The total force \mathbf{F}_i , and momentum \mathbf{M}_i acting on particle i are obtained as sums of the pair-wise interaction of particle i with its N_c contacting neighbors.

The numerical implementation of the rotational degree of freedom deserves a better description. It is noticeable that the set of Eqs. (17) is the first step to calculate the evolution of the particles angular velocity ω , in the body frame. However, a second step is necessary to solve for the particle orientation, which is necessary to model non-spherical particles. Furthermore, the rotational part of the motion equations is represented by using a quaternion representation, due to its several demonstrated technical advantages. So that, the unit quaternion $\mathbf{q} = (q_0, q_1, q_2, q_3) = q_0 + q_1i + q_2j + q_3k$ characterizes the particle orientation^{50,51} where $\sum_{i=0}^3 q_i^2 = 1$. CUDA thrust device functions have been implemented to integrate the 3D equation of motions. Details of this implementation can be found in Refs. 26 and 45.

To model hard particles, the maximum overlap must always be much smaller than the particle size. This has been ensured by introducing values for normal elastic constant, $k_n = 2.8 \times 10^6$ N/m.

Moreover, we used equivalent normal dissipation parameter $\gamma_n = \sqrt{(4k_n m_{12}) / ((\frac{\pi}{\ln 1/\alpha})^2 + 1)} \text{ s}^{-1}$, that corresponds with specific value of the normal α . For the case of linear-spot model, the collision time can be estimated, $t_c = \pi \sqrt{m_{12}/k_n}$, accordingly a time $\Delta t = t_c/50$ has been used. It is important to clarify that presupposing a constant restitution coefficient is not always valid when using DEMs of non-spherical particles, due to the dependence of the energy loss on the type of collision. However, to compare the numerical simulations with existing analytical predictions of kinetic theory, systems of rods with contact parameters equivalent to restitution coefficients $\alpha = 0.90$ and 0.95 were studied. Moreover, to check the effect of the composition we explore systems with $[\beta = 0.0; 0.25; 0.5; 0.75; 1.0]$. Simulations are computed using rods of different aspect ratios, $\xi = [1.25 - 4]$, keeping the packing fraction equal to $\eta_r = 0.007$. Although no data are included in this report, similar results are found with $\eta_r = 0.045$.

IV. RESULTS AND DISCUSSION

The cooling dynamics of mixtures composed of frictionless rods and spheres was numerically explored. As pointed out above, our system consisted of $N_R = \beta N$ rods and $N_S = (1 - \beta)N_R$ spheres, which were randomly placed in the space domain, at the beginning of the process. We explored systems with system size $N = [512; 4096; 32\,768]$ grains. Moreover, random angular and translational velocities were initially assigned to the particles. We performed preliminary studies exploring the system behavior using different initial conditions for the particle velocity distributions. Then, we selected characteristic values of the initial velocity distributions, so that the mechanical energy per particle in each degree of freedom was the same. This state corresponds to $T_R(0) = \theta(0) = \beta N$ and $T_S = (1 - \beta)N$. Note that these values do not necessarily equal the expected at the long term limit. Thus, it allowed us to clarify the system evolution to a normal state, in which all temperature ratios are constant in time.

The energy decay of freely evolving mixtures is studied, monitoring the marginal translational $T_R(t)$ and $T_S(t)$ and rotational $\theta(t)$ kinetic energies per particle. First, the relative decrease of the translational kinetic energies of both species ($T_R(t)$ and $T_S(t)$) is examined. Fig. 3 illustrates the behavior of the ratio between the two translational temperatures $\frac{T_R}{T_S}(t)$. The generality of our findings is clarified, investigating systems of spheres and rods with different aspect ratios. Additionally, several mixture compositions are explored. From the results of Fig. 3, it is evident that the systems start from a state where the relative amount of energy accumulated by each component is not in steady conditions. However, multiple collisions lead to an efficient energy interchange between species. Hence, while the system total energy diminishes, the remaining energy is redistributed among the two species. As it can be appreciated, the energy sharing occurs in such a way that the value of $\frac{T_R}{T_S}(t)$ converges to a *plateau*, indicating a trend consistent with a normal solution. In addition, it denotes the strong correlation of the cooling of both species $\frac{T_R}{T_S}(\infty) = 1$. These results show that after reaching the *plateau* the system translation energy cools down uniformly, while the marginal translational kinetic energies, $T_R(t)$ and $T_S(t)$, diminish with the same rate. Indeed, after a transient, $T_R(t)$ and $T_S(t)$ are very similar, which suggests the existence of a regime where the gas remains very well mixed denoting “*thermal equilibrium*” between species. Thus, for the time regimes considered here, the cooling dynamics is totally controlled by energy dissipation during single collisions between particles. The species interact between them sharing energy and, as a result, the translational energy per particle of each component becomes equalized and continues to decrease with the same rate.

As second step, we examine the way the energy is stored and shared within the rods’ internal degrees of freedom. In Fig. 4, the evolution of the ratio between the rotational $\theta(t)$ and translational $T_R(t)$ kinetic energies of the rods is shown. It is noticeable that again there are two different cooling regimes. Initially, one observes a transient regime where the $\frac{\theta}{T_R}(\infty)$ is not constant. However, while the rods’ total energy decreases, it is quickly redistributed among $T_R(t)$ and $\theta(t)$. This process leads to a constant value of $\frac{\theta}{T_R}(\infty)$, which is in better agreement with full energy equipartition $\frac{\theta}{T_R}(\infty) = \frac{2}{3}$, when the aspect ratio of the rods is large.

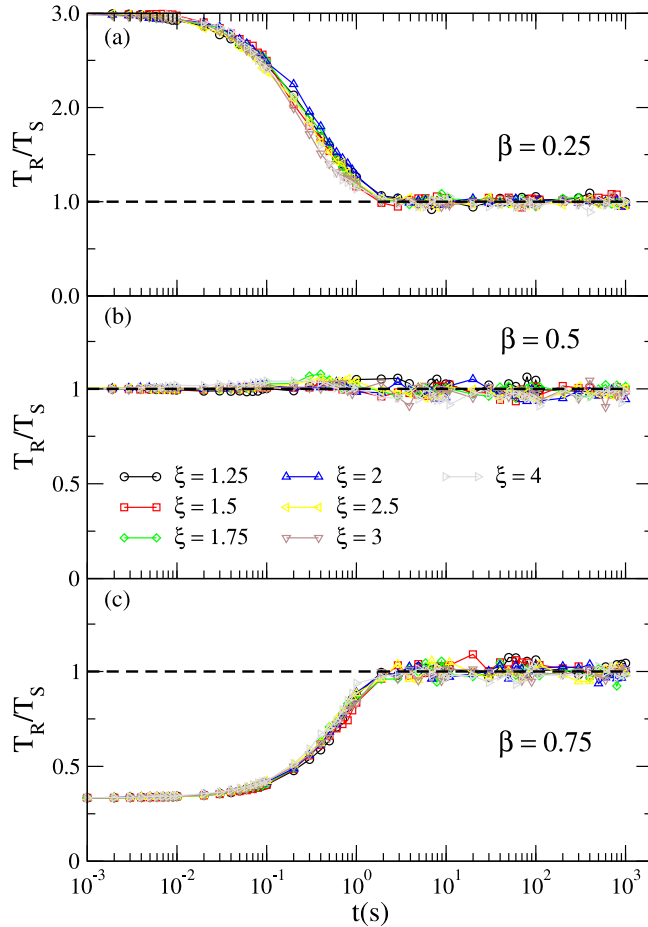


FIG. 3. Evolution of the ratio between the granular temperatures of the two components T_R/T_S vs time. Outcomes obtained for different compositions are illustrated [(a) $\beta = 0.25$, (b) $\beta = 0.5$ and (c) $\beta = 0.75$].

Nevertheless, in systems composed of spheres and short rods $\xi < 1.5$, deviations from full energy equipartition are more noticeable, regardless of mixture composition. In these cases, the rods do not equally share their energy among degrees of freedom and, consequently, the asymptotic value $\frac{\theta}{T_R}(\infty)$ depends slightly on both aspect ratio and mixture composition $\frac{\theta}{T_R}(\infty) = f(\xi, \beta)$. These outcomes suggest that energy interchange between the rotational and translational degrees of freedom is notably affected for particles with $\xi < 1.5$. In fact, $\theta(t)$ stores more energy than $T_R(t)$, as shown by the fact that $\frac{\theta}{T_R}(\infty) > \frac{2}{3}$. While these observations are non-trivial, it can be expected that below a threshold value of the elongation ξ_c , a single collision of two rods might favor the translational to rotational energy transfer. Indeed, in a collision of two rods where the contact point is very close to the center of mass of one of the rods, its translational energy diminishes while its rotational movement is less affected. Moreover, the continuous energy dissipation induces the decrease of the collision frequency and, as a result, this weak symmetric breaking mechanism unbalances the energy interchange process. Moreover, this effect is enhanced as the rods get shorter, because this type of collision occurs more frequently. This trend was earlier reported, while studying the free cooling of monodisperse ellipsoids^{25,26} and rods.⁴⁵

Fig. 5 illustrates the temporal dependence of the ratio between the marginal translational temperature of the rods $T_R(t)$ and the total temperature $T(t)$, defined by Eq. (1). Remarkably, after a short transient, $\frac{T_R}{T}(t)$ converges to its corresponding analytical value of Eq. (14), which describes its dependence of the mixture composition β assuming full energy equipartition among all degrees of freedom. Thus, free cooling granular mixtures reach an asymptotic long-time homogeneous cooling behavior, where the energy distribution among degrees of freedom remains invariant. Moreover,

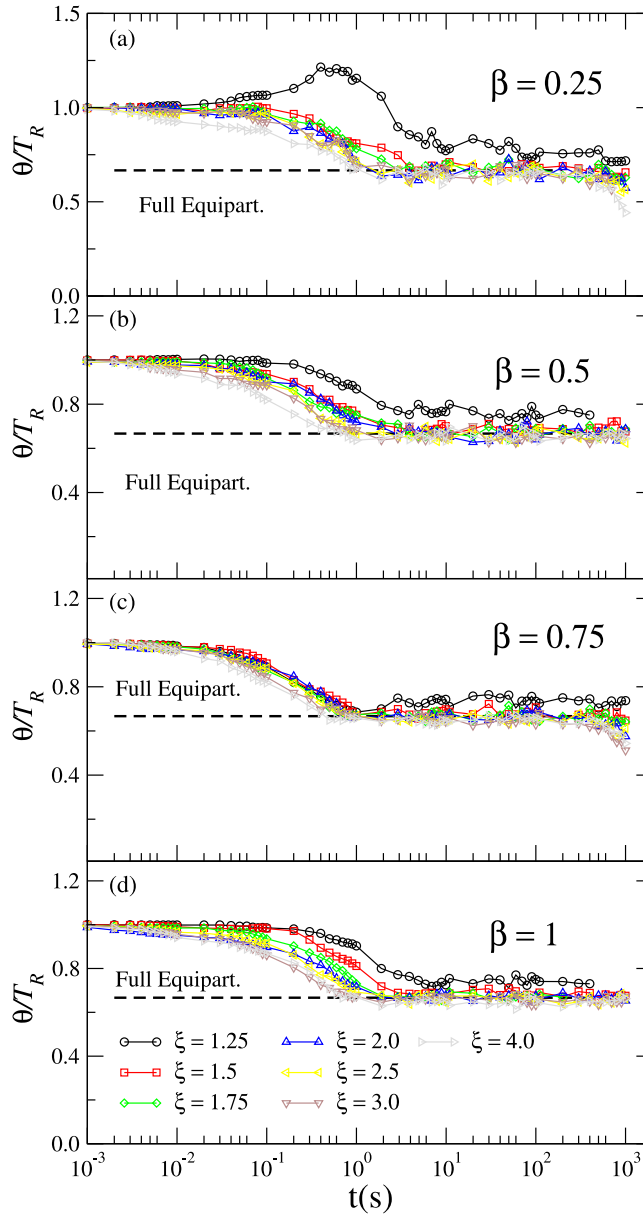


FIG. 4. Evolution of the ratio between the marginal rotational θ and translational T_R granular temperatures of the rods vs time. Outcomes obtained for different compositions are illustrated [(a) $\beta = 0.25$, (b) $\beta = 0.5$, (c) $\beta = 0.75$ and (d) $\beta = 1.0$]. For comparison, the expected result assuming energy equipartition $\frac{\theta}{T_R} = \frac{2}{3}$ is shown.

in systems composed of spheres and rods with $\xi > 1.5$, the amount of energy stored by each component of the mixture only depends on mixture composition β .

In Fig. 6, we represent the evolution in time of the granular temperature $\frac{T(t)}{T(0)}$, obtained for mixtures of spheres and rods with different elongations. As expected from the previous observations in weak dissipative systems, the ensemble of particles uniformly reduces its temperature, reaching a homogeneous cooling regime. The granular temperature $T(t)$ is compared to the analytical prediction of Eq. (4). Note, in each case the real simulation time is rescaled with its corresponding analytical prefactor, resulting in a time scale $\tau(\xi, \beta) = \frac{(1-\alpha^2)}{2} n \tilde{\Gamma}_o(\xi, \beta) \sqrt{\frac{T(0)}{m}} t$, where $\tilde{\Gamma}_o(\xi, \beta)$ is defined by Eq. (15), where $\mathcal{D}_{RS}(\xi)$ is used as fitting parameter, comparing the numerical data of $\frac{T(t)}{T(0)}$ with Haff's law. Recall that $\mathcal{D}_{RS}(\xi)$ and $\mathcal{D}_{RR}(\xi)$ in Eq. (15) quantify the efficiency of

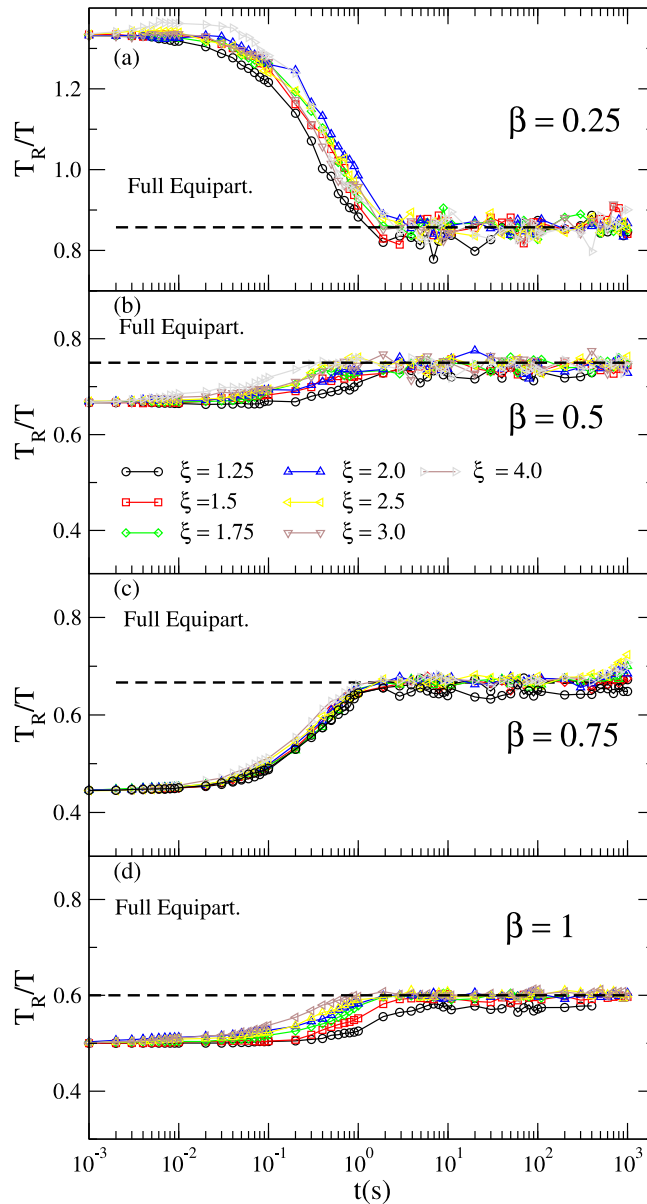


FIG. 5. Evolution of the ratio between the translational temperatures T_R of the rods and the total temperature of the mixture. Outcomes obtained for different compositions are illustrated [(a) $\beta = 0.25$, (b) $\beta = 0.5$, (c) $\beta = 0.75$ and (d) $\beta = 1$]. For comparison, it is shown the expected result $\frac{T_R}{T} = \frac{1}{(1-\beta) + \frac{5}{3}\beta}$, assuming equipartition.

the energy transfer between rotational and translation degrees of freedom for collisions between sphere-rod and rod-rod, respectively. $\mathcal{D}_{RR}(\xi)$ is identical to that obtained (assuming equipartition) for a monodisperse granular gas composed of rods, i.e., the limiting case $\beta = 1$.⁴⁵

The data collapse (see Fig. 6), in a wide domain of aspect ratio $\xi = [1.25 - 4.0]$, and the excellent agreement with the analytical prediction are noticeable. Remarkably, we found a homogeneous cooling regime, where energy of the system uniformly diminishes and the time dependency of all intensive properties is described by the granular temperature $T(t)$. Furthermore, our numerical outcomes are in good agreement with a mean field theory introduced in Section II, and the relevant time scale of the cooling process is mainly determined by the mixture composition β and particle elongation ξ .

Fig. 7 shows the values of $\mathcal{D}_{RS}(\xi)$ and $\mathcal{D}_{RR}(\xi)$ obtained from the collapse of all the curves and their comparison with Haff's law. For sake of simplicity, the data values are given in terms of $4\pi\sigma^2$

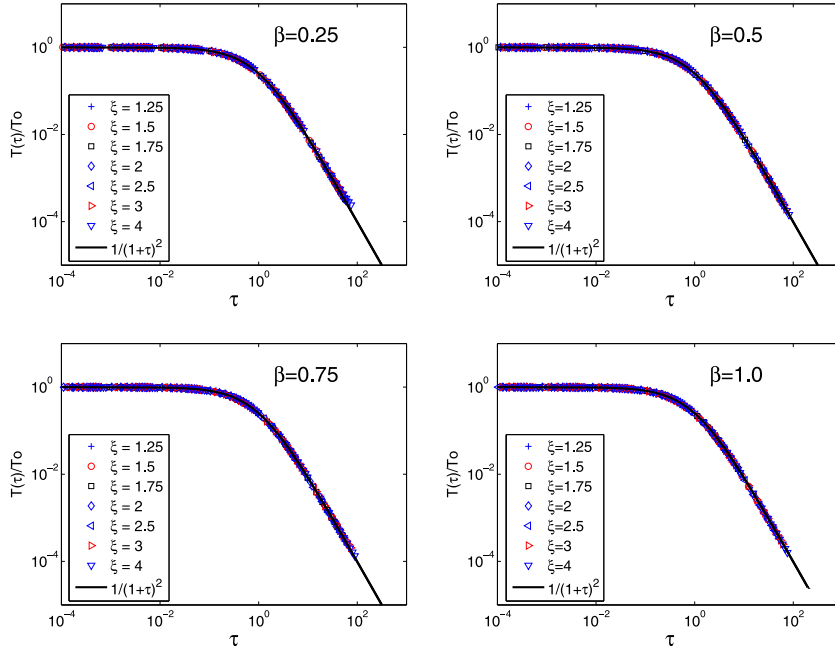


FIG. 6. Evolution of the granular temperature $T(\tau)/T(0)$, defined as Eq. (1) vs the characteristic time τ , note the scaling of all the curves when using the characteristic time $\tau(\xi) = \frac{(1-\alpha^2)}{2} n \bar{\Gamma}_o \sqrt{\frac{T(0)}{m}} t$. The numerical data corresponding to particles with different elongations and restitution coefficient ($\alpha = 0.90$) are included. Outcomes obtained for different compositions are illustrated [$\beta = 0.25, \beta = 0.5, \beta = 0.75$ and $\beta = 1.0$].

(see Eq. (15)), i.e., the surface of a sphere with the same volume. Recall that $\mathcal{D}_{RS}(\xi)$ quantifies the efficiency of the energy transfer between rotational and translation degrees of freedom, as well as, its particle’s size dependence, in collisions between spheres and rods with the same mass and volume. As we pointed out earlier, this procedure allows us to numerically determine $\mathcal{D}_{RS}(\xi)$. Note, the values of $\mathcal{D}_{RS}(\xi)$ and $\mathcal{D}_{RR}(\xi)$ are obtained comparing the numerical data of the granular temperature $\frac{T(t)}{T(0)}$, with the analytical formula Eq. (4), using the time scale $\tau(\xi, \beta)$ and fitting a single parameter $\mathcal{D}_{RS}(\xi)$. We found that the values of $\mathcal{D}_{RS}(\xi)$ are smaller than their corresponding

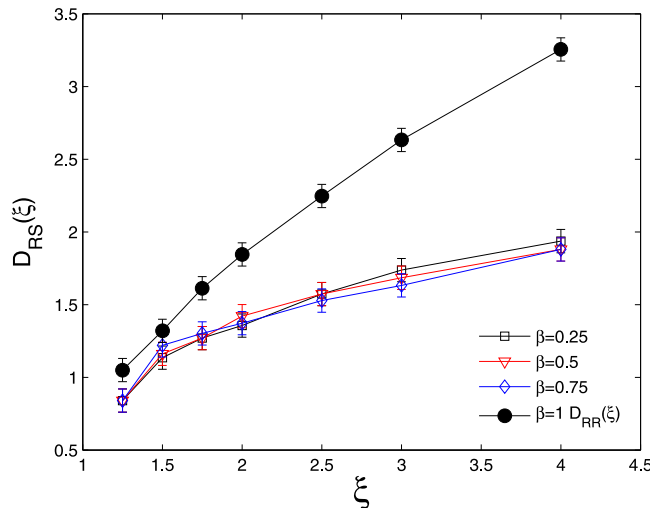


FIG. 7. Values of the numerical estimation of $\mathcal{D}_{RS}(\xi)$, obtained collapsing each numerical data (see Fig. 6) of the total temperature $\frac{T(t)}{T(0)}$ and its corresponding analytic prediction of Eq. (4).

$\mathcal{D}_{RR}(\xi)$ values. As expected $\mathcal{D}_{RS}(\xi)$ does not depend on the mixture composition β , within our numerical uncertainties. Our outcomes suggest that regardless of particle's elongation the energy transfer between degrees of freedom is less efficient in rod-sphere collisions in comparison with rod-rod collisions.

In conclusion, we theoretically investigated the cooling dynamics of a binary mixture of frictionless spherical particles and rods. A generalized mean field analytical theory accounting for the cooling dynamics of the mixture has been formulated. Complementarity, using a hybrid GPU-CPU architecture, we have numerically explored a HCS of dilute granular mixtures composed by 3D of spherocylindrical particles and spheres with the same volume. Regardless of the particle shape, we have numerically found that the cooling process has two stages. First, a transient regime is observed, but in general the granular temperature of each species quickly decays towards a final state where the remaining energy is equally redistributed among the degrees of freedom of the two species. Hence, while the system temperature diminishes, there is energy balance between species and the ratio between the translational kinetic energy of the two species $\frac{T_R}{T_S}(\infty) \approx 1$ is maintained. Meanwhile, in this final state the ratio of the energy corresponding to the internal degrees of freedom of the rods is a constant value $\frac{\theta}{T_R}(\infty)$. We obtained that increasing the rods' aspect ratio, the energy equipartition is notably favored $\frac{\theta}{T_R}(\infty) \approx \frac{2}{3}$. Moreover, we found that regardless of the initial conditions, multiple collisions lead to a quick energy interchange between species, which suggests that the memories effect are very weak. That is also supported by the fact that similar outcomes were attained with a much higher volume fraction $\eta_r = 0.045$ (actual value $\eta_r = 0.007$). Furthermore, we use the scaling properties of the HCS to obtain numerically the functional form of $\mathcal{D}_{RS}(\xi)$. This quantity controls the energy transfer between rotational and translation degrees of freedom, in collisions between spheres and rods with the same mass and volume. Note that $\mathcal{D}_{RS}(\xi)$ is a key ingredient, when analytically examining the mixture cooling kinetics and, unfortunately, this has not been analytically calculated, so far. Finally, we anticipate that introducing particle friction has a significant influence on the mixture cooling kinetics, due to the fact that rod's azimuthal and polar rotational degrees of freedom evolve with different characteristic times. These issues will be investigated in future works.

ACKNOWLEDGMENTS

This work began while the author R. C. Hidalgo was visiting the Institut für Multiskalensimulation, Friedrich-Alexander-Universität Erlangen-Nürnberg; its financial support and hospitality are gratefully acknowledged. The Spanish MINECO (Project No. FIS2014-57325) have supported this work. The German Science Foundation (DFG) is acknowledged for funding through the Cluster of Excellence Engineering of Advanced Materials. The authors thank S. McNamara for proofreading the manuscript.

APPENDIX: EVALUATION OF THE COOLING COEFFICIENT

In order to evaluate Γ (cf. Eq. (3)), it is sufficient to consider the following integral:

$$\zeta_{12} = \int f_1(\mathbf{u}_1, \omega_1, \gamma_1) f_2(\mathbf{u}_2, \omega_2, \gamma_2) |\mathbf{u}_{12}| \Delta E_{12} ds_{12} d\mathbf{u}_1 d\mathbf{u}_2 d\omega_1 d\omega_2 d\gamma_1 d\gamma_2, \quad (\text{A1})$$

corresponding to the cooling rate due to collisions between two smooth biaxial rigid bodies "1" and "2," with the infinitesimal cross section ds_{12} given by the relation,^{42,43}

$$|\mathbf{u}_{12}| ds_{12} = (\mathbf{c}_{12} \cdot \mathbf{n}) S(\mathbf{n}, \gamma_1, \gamma_2) d\mathbf{n},$$

where $S_{12}(\mathbf{n}, \gamma_1, \gamma_2) d\mathbf{n}$ is the infinitesimal surface element on the excluded volume of the colliding bodies. Substituting the change of energy ΔE_{12} in Eq. (A1), using Eqs. (9) and (10), and defining

$$\begin{aligned} \tilde{\omega}_1^2 &\equiv \frac{I_1}{\theta_1} \omega_1^2, \\ \tilde{u}_{12}^2 &\equiv \frac{3m}{2(T_{R1} + T_{R2})} u_{12}^2, \end{aligned}$$

and

$$\tilde{u}_c^2 \equiv \frac{3m(T_{R_2}\mathbf{u}_1 + T_{R_1}\mathbf{u}_2)^2}{2(T_{R_1} + T_{R_2})^3},$$

one obtains

$$\begin{aligned} \zeta_{12} = & -\frac{(1 - \alpha^2)}{2\pi^5} \frac{1}{\Omega^2} \frac{(T_{R_1} + T_{R_2})^3}{T_{R_1}^{\frac{3}{2}} T_{R_2}^{\frac{3}{2}}} \int e^{-\left(\frac{T}{T_{R_1} + T_{R_2}}\right)^2 \tilde{u}_c^2 - \tilde{u}_{12}^2 - \tilde{\omega}_1^2 - \omega_2^2} (\mathbf{c}_{12} \cdot \mathbf{n})^3 \\ & \times S(\mathbf{n}, \gamma_1, \gamma_2) d\mathbf{n} d\tilde{\mathbf{u}}_c d\tilde{\mathbf{u}}_{12} d\tilde{\omega}_1 d\tilde{\omega}_2 d\gamma_1 d\gamma_2. \end{aligned}$$

The integral over $\tilde{\mathbf{u}}_c$ and the components of $\tilde{\mathbf{u}}_{12}$ in the plane perpendicular to \mathbf{n} can readily be performed to yield

$$\begin{aligned} \zeta_{12} = & -\frac{1}{\Omega^2} \frac{(1 - \alpha^2)}{2\pi^{\frac{5}{2}}} \int e^{-\tilde{\mathbf{u}}_{12} \cdot \mathbf{n})^2 - \tilde{\omega}_1^2 - \omega_2^2} \mu(\mathbf{r}_1, \mathbf{r}_2, \mathbf{n}) (\mathbf{c}_{12} \cdot \mathbf{n})^3 \\ & \times S(\mathbf{n}, \gamma_1, \gamma_2) d\mathbf{n} d(\tilde{\mathbf{u}}_{12} \cdot \mathbf{n}) d\tilde{\omega}_1 d\tilde{\omega}_2 d\gamma_1 d\gamma_2. \end{aligned}$$

Next, following Ref. 44 build the 5 dimensional vector $(\tilde{\omega}_1, \tilde{\omega}_2, \tilde{g})$ and perform an orthogonal linear transformation

$$(\tilde{\omega}_1, \tilde{\omega}_2, \tilde{g}) \rightarrow \tilde{\xi} = (\tilde{\xi}_1, \tilde{\xi}_2, \tilde{\xi}_3),$$

where $\tilde{g} \equiv \tilde{\mathbf{u}}_{12} \cdot \mathbf{n}$, so that one of the unit vectors $\hat{\boldsymbol{\varepsilon}}$ of the rotated frame verifies

$$\begin{aligned} \tilde{\xi} \cdot \hat{\boldsymbol{\varepsilon}} & \propto \tilde{c}, \\ \hat{\boldsymbol{\varepsilon}} \cdot \hat{\boldsymbol{\varepsilon}} & = 1, \end{aligned}$$

where

$$\tilde{c} \equiv \sqrt{\frac{3m}{2(T_{R_2} + T_{R_1})}} (\mathbf{c}_{12} \cdot \mathbf{n}).$$

The vector $\hat{\boldsymbol{\varepsilon}}$ is given by

$$\hat{\boldsymbol{\varepsilon}} = \frac{1}{\tilde{D}} \left(\sqrt{\frac{3m}{2I_1} \frac{\theta_1}{T_{R_2} + T_{R_1}}} \mathbf{a}_1, \sqrt{\frac{3m}{2I_2} \frac{\theta_2}{T_{R_2} + T_{R_1}}} \mathbf{a}_2, 1 \right),$$

where $\mathbf{a}_1 \equiv (\mathbf{r}_1 \times \mathbf{n})$, $\mathbf{a}_2 \equiv -(\mathbf{r}_2 \times \mathbf{n})$, and

$$\tilde{D}^2 = 1 + \frac{3m}{2I_1} \frac{\theta_1}{T_{R_2} + T_{R_1}} (\mathbf{r}_1 \times \mathbf{n})^2 + \frac{3m}{2I_2} \frac{\theta_2}{T_{R_2} + T_{R_1}} (\mathbf{r}_2 \times \mathbf{n})^2.$$

One has $\tilde{\xi} \cdot \hat{\boldsymbol{\varepsilon}} = \frac{\tilde{c}}{\tilde{D}}$, so that

$$\begin{aligned} \zeta_{12} = & -\frac{1}{\Omega^2} \frac{(1 - \alpha^2)}{2\pi^{\frac{7}{2}}} \left(\frac{3m}{2T} \frac{T}{T_{R_2} + T_{R_1}} \right)^{-\frac{3}{2}} \int e^{-\tilde{\xi}_1^2 + \tilde{\xi}_2^2 + \tilde{\xi}_3^2} \mu(\mathbf{r}_1, \mathbf{r}_2, \mathbf{n}) \tilde{D}^3 (\tilde{\xi} \cdot \hat{\boldsymbol{\varepsilon}})^3 \\ & \times S(\mathbf{n}, \gamma_1, \gamma_2) d\mathbf{n} d\tilde{\xi}_1 d\tilde{\xi}_2 d\tilde{\xi}_3 d\gamma_1 d\gamma_2. \end{aligned}$$

Performing the integration over $\tilde{\xi}_1, \tilde{\xi}_2$, and $\tilde{\xi}_3$ yields

$$\begin{aligned} \zeta_{12} = & -\frac{2}{9} \frac{\sqrt{3}}{\sqrt{\pi}} (1 - \alpha^2) \frac{T^{\frac{3}{2}}}{\sqrt{m}} \left(\frac{T_{R_2} + T_{R_1}}{2T} \right)^{\frac{3}{2}} \frac{1}{\Omega^2} \int \frac{\left(1 + \frac{3m}{2I_1} \frac{\theta_1}{T_{R_2} + T_{R_1}} (\mathbf{r}_1 \times \mathbf{n})^2 + \frac{3m}{2I_2} \frac{\theta_2}{T_{R_2} + T_{R_1}} (\mathbf{r}_2 \times \mathbf{n})^2 \right)^{\frac{3}{2}}}{1 + \left(\frac{m}{2I_1} (\mathbf{r}_1 \times \mathbf{n})^2 + \frac{m}{2I_2} (\mathbf{r}_2 \times \mathbf{n})^2 \right)} \\ & \times S(\mathbf{n}, \gamma_1, \gamma_2) d\mathbf{n} d\gamma_1 d\gamma_2. \end{aligned}$$

Using the above expression to evaluate the three contributions in Eq. (3) yields expression (11) for the cooling coefficient Γ (where notice that a factor 1/2 multiplies the rod-rod and sphere-sphere contributions to avoid double counting).

- ¹ T. Pöschel and S. Luding, *Granular Gases* (Springer-Verlag, Berlin, Heidelberg, Germany, 2001).
- ² N. V. Brilliantov and T. Pöschel, *Kinetic Theory of Granular Gases* (Oxford University Press, Oxford, UK, 2004).
- ³ S. Tatsumi, Y. Murayama, H. Hayakawa, and M. Sano, “Experimental study on the kinetics of granular gases under microgravity,” *J. Fluid Mech.* **641**, 521 (2009).
- ⁴ K. Nichol and K. E. Daniels, “Equipartition of rotational and translational energy in a dense granular gas,” *Phys. Rev. Lett.* **108**, 018001 (2012).
- ⁵ A. Sack, M. Heckel, J. E. Kollmer, F. Zimmer, and T. Pöschel, “Energy dissipation in driven granular matter in the absence of gravity,” *Phys. Rev. Lett.* **111**, 018001 (2013).
- ⁶ L. J. Daniels, Y. Park, T. C. Lubensky, and D. J. Durian, “Dynamics of gas-fluidized granular rods,” *Phys. Rev. E* **79**, 041301 (2009).
- ⁷ K. Harth, U. Kornek, T. Trittel, U. Strachauer, S. Höme, K. Will, and R. Stannarius, “Granular gases of rod-shaped grains in microgravity,” *Phys. Rev. Lett.* **110**, 144102 (2013).
- ⁸ K. Harth, T. Trittel, K. May, S. Wegner, and R. Stannarius, “Three-dimensional (3D) experimental realization and observation of a granular gas in microgravity,” *Adv. Space Res.* **55**, 1901 (2015).
- ⁹ J. J. Brey, M. J. Ruiz-Montero, and D. Cubero, “Homogeneous cooling state of a low-density granular flow,” *Phys. Rev. E* **54**, 3664 (1996).
- ¹⁰ J. J. Brey, F. Moreno, and J. W. Dufty, “Model kinetic equation for low-density granular flow,” *Phys. Rev. E* **54**, 445 (1996).
- ¹¹ N. V. Brilliantov, F. Spahn, J. M. Hertzsch, and T. Pöschel, “Model for collisions in granular gases,” *Phys. Rev. E* **53**, 5382 (1996).
- ¹² S. Luding, in *Physics of Dry Granular Media*, edited by H. J. Herrmann, J.-P. Hovi, and S. Luding, NATO ASI Series E Vol. 350 (Kluwer Academic Publishers, Dordrecht, 1998), pp. 285–304.
- ¹³ P. Haff, “Grain flow as a fluid-mechanical phenomenon,” *J. Fluid Mech.* **134**, 401 (1983).
- ¹⁴ N. V. Brilliantov and T. Pöschel, “Velocity distribution in granular gases of viscoelastic particles,” *Phys. Rev. E* **61**, 5573 (2000).
- ¹⁵ A. Puglisi, V. Loreto, U. M. B. Marconi, A. Petri, and A. Vulpiani, “Clustering and non-Gaussian behavior in granular matter,” *Phys. Rev. Lett.* **81**, 3848 (1998).
- ¹⁶ S. Luding and S. McNamara, “How to handle the inelastic collapse of a dissipative hard-sphere gas with the TC model,” *Granular Matter* **1**, 113 (1998).
- ¹⁷ X. Nie, E. Ben-Naim, and S. Chen, “Dynamics of freely cooling granular gases,” *Phys. Rev. Lett.* **89**, 204301 (2002).
- ¹⁸ S. Miller and S. Luding, “Cluster growth in two- and three-dimensional granular gases,” *Phys. Rev. E* **69**, 031305 (2004).
- ¹⁹ S. Luding, M. Huthmann, S. McNamara, and A. Zippelius, “Homogeneous cooling of rough, dissipative particles: Theory and simulations,” *Phys. Rev. E* **58**, 3416 (1998).
- ²⁰ N. V. Brilliantov, T. Pöschel, W. T. Kranz, and A. Zippelius, “Translations and rotations are correlated in granular gases,” *Phys. Rev. Lett.* **98**, 128001 (2007).
- ²¹ W. Kranz, N. Brilliantov, T. Pöschel, and A. Zippelius, “Correlation of spin and velocity in the homogeneous cooling state of a granular gas of rough particles,” *Eur. Phys. J.: Spec. Top.* **179**, 91 (2009).
- ²² A. Santos, G. M. Kremer, and V. Garzó, “Energy production rates in fluid mixtures of inelastic rough hard spheres,” *Prog. Theor. Phys. Suppl.* **184**, 31 (2010).
- ²³ M. Huthmann, T. Aspelmeier, and A. Zippelius, “Granular cooling of hard needles,” *Phys. Rev. E* **60**, 654 (1999).
- ²⁴ T. Aspelmeier, G. Giese, and A. Zippelius, “Cooling dynamics of a dilute gas of inelastic rods: A many particle simulation,” *Phys. Rev. E* **57**, 857 (1998).
- ²⁵ F. Villemot and J. Talbot, “Homogeneous cooling of hard ellipsoids,” *Granular Matter* **14**, 91 (2012).
- ²⁶ S. M. Rubio-Largo, P. G. Lind, D. Maza, and R. C. Hidalgo, “Granular gas of ellipsoids: Analytical collision detection implemented on GPUs,” *Comput. Part. Mech.* **2**, 127 (2015).
- ²⁷ G. Costantini, U. Marini Bettolo Marconi, G. Kalibaeva, and G. Ciccotti, “The inelastic hard dimer gas: A nonspherical model for granular matter,” *J. Chem. Phys.* **122**, 164505 (2005).
- ²⁸ T. Kanzaki, R. C. Hidalgo, D. Maza, and I. Pagonabarraga, “Cooling dynamics of a granular gas of elongated particles,” *J. Stat. Mech.* **2010**, P06020.
- ²⁹ J. M. Ottino and D. V. Khakhar, “Mixing and segregation of granular materials,” *Annu. Rev. Fluid Mech.* **32**, 55 (2000).
- ³⁰ T. Shinbrot and F. J. Muzzio, “Nonequilibrium patterns in granular mixing and segregation,” *Phys. Today* **53**(3), 25 (2000).
- ³¹ A. Kudrolli, “Size separation in vibrated granular matter,” *Rep. Prog. Phys.* **67**, 209 (2004).
- ³² A. Rosato, K. J. Strandburg, F. Prinz, and R. H. Swendsen, “Why the Brazil nuts are on top: Size segregation of particulate matter by shaking,” *Phys. Rev. Lett.* **58**, 1038 (1987).
- ³³ J. T. Jenkins and F. Mancini, “Balance laws and constitutive relations for plane flows of a dense, binary mixture of smooth, nearly elastic, circular disks,” *J. Appl. Mech.* **54**, 27 (1987).
- ³⁴ D. Serero, S. H. Noskowitz, and I. Goldhirsch, “Exact results versus mean field solutions for binary granular gas mixtures,” *Granular Matter* **10**, 37 (2007).
- ³⁵ J. M. Montanero and V. Garzó, “Monte Carlo simulation of the homogeneous cooling state for a granular mixture,” *Granular Matter* **4**, 17 (2002).
- ³⁶ V. Garzó and J. Dufty, “Homogeneous cooling state for a granular mixture,” *Phys. Rev. E* **60**, 5706 (1999).
- ³⁷ A. Barrat and E. Trizac, “Lack of energy equipartition in homogeneous heated binary granular mixtures,” *Granular Matter* **4**, 57 (2002).
- ³⁸ S. R. Dahler, C. M. Hrenya, V. Garzó, and J. W. Dufty, “Kinetic temperatures for a granular mixture,” *Phys. Rev. E* **66**, 041301 (2002).
- ³⁹ I. Goldhirsch, S. H. Noskowitz, and O. Bar-Lev, “The homogeneous cooling state revisited,” *Lect. Notes Phys.* **624**, 37 (2003).
- ⁴⁰ M. Huthmann and A. Zippelius, “Dynamics of inelastically colliding rough spheres: Relaxation of translational and rotational energy,” *Phys. Rev. E* **56**, R6275 (1997).

- ⁴¹ I. Goldhirsch, S. H. Noskowitz, and O. Bar-Lev, "Nearly smooth granular gases," *Phys. Rev. Lett.* **95**, 068002 (2005).
- ⁴² C. F. Curtiss, "Kinetic theory of nonspherical molecules," *J. Chem. Phys.* **24**, 225 (1956).
- ⁴³ C. F. Curtiss and J. S. Dahler, "Kinetic theory of nonspherical molecules. V," *J. Chem. Phys.* **38**, 2352 (1963).
- ⁴⁴ D. K. Hoffman, "Collision integrals of a gas of rigid convex molecules," *J. Chem. Phys.* **50**, 4823 (1969).
- ⁴⁵ S. M. Rubio-Largo, F. Alonso-Marroquí, T. Weinhart, S. Luding, and R. C. Hidalgo, "Homogeneous cooling state of frictionless rod particles," *Physica A* **443**, 477 (2016).
- ⁴⁶ R. C. Hidalgo, T. Kanzaki, F. Alonso-Marroquí, and S. Luding, "On the use of graphics processing units (GPUs) for molecular dynamics simulation of spherical particles," *AIP Conf. Proc.* **1542**, 169 (2013).
- ⁴⁷ F. Alonso-Marroquí, "Spheropolygons: A new method to simulate conservative and dissipative interactions between 2D complex-shaped rigid bodies," *Europhys. Lett.* **83**, 14001 (2008).
- ⁴⁸ F. Alonso-Marroquí and Y. Wang, "An efficient algorithm for granular dynamics simulations with complex-shaped objects," *Granular Matter* **11**, 317 (2009).
- ⁴⁹ S. A. Galindo-Torres, F. Alonso-Marroquí, Y. C. Wang, D. Pedroso, and J. D. Muñoz Castaño, "Molecular dynamics simulation of complex particles in three dimensions and the study of friction due to nonconvexity," *Phys. Rev. E* **79**, 060301 (2009).
- ⁵⁰ D. Evans, "On the representation of orientation space," *Mol. Phys.* **34**, 317 (1977).
- ⁵¹ D. Evans and S. Murad, "Singularity free algorithm for molecular dynamics simulation of rigid polyatomics," *Mol. Phys.* **34**, 327 (1977).